The Journal of Nutrition
Nutrition and Disease

PPARα Expression Protects Male Mice from High Fat–Induced Nonalcoholic Fatty Liver[1–3]

Mohamed A. Abdelmegeed,[4] Seong-Ho Yoo,[4] Lauren E. Henderson,[4] Frank J. Gonzalez,[5] Kimberley J. Woodcroft,[6] and Byoung-Joon Song[4]*

[4]Laboratory of Membrane Biochemistry and Biophysics, National Institute on Alcohol Abuse and Alcoholism, and [5]Laboratory of Metabolism, National Cancer Institute, National Institutes of Health, Bethesda, MD 20892; and [6]Biostatistics and Research Epidemiology, Henry Ford Health System, Detroit, MI 48202

Abstract

Emerging evidence suggests that the lack of PPARα enhances hepatic steatosis and inflammation in *Ppara*-null mice when fed a high-fat diet (HFD). Thus, the aim of this study was to determine whether *Ppara*-null mice are more susceptible to nonalcoholic steatohepatitis (NASH) than their wild-type (WT) counterparts following short-term feeding with a HFD. Age-matched male WT and *Ppara*-null mice were randomly assigned to consume ad libitum a standard Lieber-DeCarli liquid diet (STD) (35% energy from fat) or a HFD (71% energy from fat) for 3 wk. Liver histology, plasma transaminase levels, and indicators of oxidative/nitrosative stress and inflammatory cytokines were evaluated in all groups. Levels of lobular inflammation and the NASH activity score were greater in HFD-exposed *Ppara*-null mice than in the other 3 groups. Biochemical analysis revealed elevated levels of ethanol-inducible cytochrome P450 2E1 and TNFα accompanied by increased levels of malondialdehyde as well as oxidized and nitrated proteins in *Ppara*-null mice. Elevated oxidative stress and inflammation were associated with activation of c-Jun-*N*-terminal kinase and p38 kinase, resulting in increased hepatocyte apoptosis in *Ppara*-null mice fed a HFD. These results, with increased steatosis, oxidative stress, and inflammation observed in *Ppara*-null mice fed a HFD, demonstrate that inhibition of PPARα functions may increase susceptibility to high fat–induced NASH. J. Nutr. 141: 603–610, 2011.

Introduction

Nonalcoholic fatty liver diseases (NAFLD)[7] represent a hepatic metabolic syndrome (1). Obesity and diabetes are common in our aging population and are frequently associated with NAFLD, which includes nonalcoholic fatty liver (simple steatosis), nonalcoholic steatohepatitis (NASH), fibrosis, and possibly cirrhosis (2). In the US, the prevalence of NAFLD and NASH are 20% and ~3–5% of the adult population, respectively (3). The "two-hit" hypothesis postulates that steatosis primes the liver to secondary insults, including reactive oxygen/nitrogen species (ROS/RNS), gut-derived endotoxins, TNFα, and other proinflammatory cytokines (4), resulting in NASH development.

The PPAR are members of the nuclear receptor superfamily, including PPARα, PPARβ/δ, and PPARγ (5,6). Upon ligand binding, PPAR form a heterodimer with retinoid X receptor, interact with PPAR response elements in the target genes, and regulate their expression (5,6). PPARα is essential in the modulation of lipid transport and metabolism, mainly through activating mitochondrial and peroxisomal fatty acid β-oxidation pathways (5–7). In addition, PPARα seems to decrease inflammation, mainly through direct interaction with NF-κB, causing inhibition of its signaling pathway (8) or reducing the activated levels of NF-κB and subsequent inflammation (9). In fact, PPARα was reported to protect the liver from obesity-induced inflammation after feeding with a high-fat diet (HFD) for 6 mo (10). Furthermore, PPARα was implicated in the attenuation of oxidative stress in alcoholic liver disease when treated with polyenephosphatidylcholine through downregulation of ROS-generating enzymes such as ethanol-inducible cytochrome P450 2E1 (CYP2E1), acyl-CoA oxidase, and NADPH oxidase (11). We recently reported that *Ppara*-null mice subjected to fasting alone developed steatosis and increased oxidative/nitrosative stress compared with the control-fed mice (12). Thus, we hypothesized that lack of functional PPARα contributes to increased

[1] Supported by the Intramural Research Fund of the National Institute on Alcohol Abuse and Alcoholism.
[2] Author disclosures: M. A. Abdelmegeed, S. H. Yoo, L. E. Henderson, F. J. Gonzalez, K. J. Woodcroft, and B. J. Song, no conflicts of interest.
[3] Supplemental Figures 1–3 of this article are available with the online posting of this paper at jn.nutrition.org.
[7] Abbreviations used: ALT, alanine aminotransferase; AST, aspartate aminotransferase; CYP2E1, ethanol-inducible cytochrome P450 2E1; HFD, high-fat diet; iNOS, inducible NO synthase; MDA, malondialdehyde; NAFLD, nonalcoholic fatty liver disease; NAS, nonalcoholic fatty liver disease activity score; NASH, nonalcoholic steatohepatitis; Null-HFD, *Ppara*-null mice fed a high-fat liquid diet; Null-STD, *Ppara*-null mice fed a standard liquid diet; ROS, reactive oxygen species; RNS, reactive nitrosative stress; p-JNK, phospho-c-Jun kinase; p-p38 kinase, phospho-p38 kinase; Prx, peroxiredoxin; Prx-SO3, oxidized inactivated peroxiredoxin; STD; standard Lieber-DeCarli liquid diet; STE buffer, buffer containing 250 mmol/L sucrose, 50 mmol/L Tris-HCl, pH 7.5, and 1 mmol/L EDTA; thiolase, 3-ketoacyl-CoA thiolase; TUNEL, terminal deoxynucleotidyl transferase dUTP nick end labeling; WT, wild type; WT-HFD, wild-type mice fed a high-fat liquid diet; WT-STD, wild-type mice fed a standard liquid diet.
* To whom correspondence should be addressed. E-mail: bj.song@nih.gov.

Manuscript received November 10, 2010. Initial review completed December 2, 2010. Revision accepted January 5, 2011.
First published online February 23, 2011; doi:10.3945/jn.110.135210.

susceptibility to the development of NAFLD and NASH through both increased oxidative stress and inflammatory response compared with the corresponding wild-type (WT) mice. The aim of this study was to examine this hypothesis by feeding WT and *Ppara*-null mice with a HFD for 3 wk, as originally described (13), instead of feeding for 6 mo (10). Steatosis, inflammatory response, oxidative stress, and the indicators of NAFLD and NASH manifestations were monitored in both WT and *Ppara*-null mice fed a HFD or a standard liquid diet (STD).

Materials and Methods

Mice and dietary protocol. Age- and sex-matched inbred *Ppara*-null mice on 129/Svj background and WT mice (stock number 2448 from the Jackson Laboratory) were used in this study, as described (10). Male mice consumed ad libitum either an STD (containing 35% energy from fat, 47% from carbohydrates, and 18% from protein) or a HFD (71% energy derived from fat, 11% from carbohydrate, and 18% from protein) (13) for 3 wk without extra drinking water. Both HFD and STD were obtained from Dyets and freshly prepared daily. Mice (6–7 wk old; 15–20 g) were randomly assigned to 4 different groups (consisting of 3 or 4 mice/group): WT-fed an STD (WT-STD); WT-fed a HFD (WT-HFD); *Ppara*-null-fed an STD (Null-STD); and *Ppara*-null-fed a HFD (Null-HFD). All mouse experiments were approved by the NIAAA Institutional Animal Care and Use Committee and conducted humanely according to the NIH Guideline.

Histopathology analysis. The whole liver was excised and weighed immediately after mice were killed by asphyxiation. Following staining with hematoxylin and eosin, histological examination was performed with the histological scoring system for NAFLD by an experienced pathologist without knowledge of treatments (14). Briefly, the proposed NAFLD activity score (NAS) was quantified by summing scores of steatosis (0–3), lobular inflammation (0–2), and hepatocellular ballooning (0–2). NASH was defined in the cases of NAS of ≥ 5. The rest of the liver samples were frozen immediately at −80°C until analysis.

Sample preparation. Approximately 500 mg liver tissue from each mouse from 4 different groups was homogenized on ice in 5 volumes of STE buffer (containing 250 mmol/L sucrose, 50 mmol/L Tris-HCl, pH 7.5, and 1 mmol/L EDTA) with protease inhibitor and phosphatase inhibitor cocktails (Calbiochem), as described (15). Cytosolic and mitochondrial fractions were prepared as described elsewhere (12,16) by sequential centrifugation of total cell homogenates and postnuclear lysates. Mitochondrial pellets were washed with ice-cold STE buffer 3 times to remove contaminating cytosolic proteins and used as the crude mitochondrial fraction after the mitochondrial proteins were dissolved in TE buffer containing 1% CHAPS (12,16).

Determination of malondialdehyde, serum transaminases, hepatic mitochondrial 3-ketoacyl-CoA thiolase, and TNFα. Hepatic malondialdehyde (MDA) levels were determined as previously described (12) despite potential interference in the MDA measurement as discussed (17). All other measurements such as serum transaminases, hepatic mitochondrial 3-ketoacyl-CoA thiolase (thiolase), and cytosolic TNFα levels were the same as described (12,16,18).

Immunoblot analysis. Cytosolic or mitochondrial proteins (10–40 μg) were separated by 12% SDS-PAGE and subjected to immunoblot analyses performed as previously described (12). Specific antibody to thiolase was kindly provided by Dr. Nancy Braverman, Johns Hopkins University (Baltimore, MD). Respective antibodies for CYP2E1, inducible NO synthase (iNOS), 3-nitrotyrosine, and GAPDH were purchased from Abcam. Antibody to oxidized peroxiredoxin (Prx) Prx-SO_3 was obtained from LabFrontier and the specific antibody to phospho-c-Jun kinase (p-JNK) or phospho-p38 kinase (p-p38 kinase) was from Cell Signaling Technology. Antibody to the mitochondrial complex II (succinate-quinone reductase) subunit was purchased from Mitosciences. After removal of the primary antibodies followed by washing steps, the nitrocellulose membranes were incubated with secondary goat anti-mouse (anti-3NT) or goat anti-rabbit (anti-thiolase, -CYP2E1, -iNOS, -Prx-SO3, p-JNK, and p-p38 kinase, respectively) conjugated with HRP (1:5000 dilutions in 5% milk powder in TE-buffered saline with 0.05% Tween 20). Protein bands were detected by enhanced chemiluminescence and their densities quantified using UN-SCAN-IT gel version 6.1 from Silk Scientific (12).

Terminal deoxynucleotidyl transferase dUTP nick end labeling (TUNEL) assay. The ApopTag peroxidase in situ apoptosis detection kit (Millipore) was used to identify apoptotic hepatocytes by labeling and detecting DNA strand breaks by the TUNEL method following the manufacturer's protocol.

Data analysis. The number of mice used was 3 WT-STD and 4 for all other groups. All statistical analyses were performed using SAS 9.2 Software (SAS Institute). Fisher's exact test was used to assess statistical differences for histological data and TUNEL assay. Two-way ANOVA was performed to assess differences in all other results. When 2-way ANOVA indicated the presence of a genotype-diet interaction, 1-way ANOVA followed by the post hoc Tukey's Studentized range test at a significance level of 0.05 was performed to determine differences among the 4 groups of mice. Equality of variances was assessed by the Modified Levene test (Brown and Forsythe test) and variances were found to be homogeneous. Reproducibility of the data were confirmed by 2 or 3 separate experiments.

Results

Histopathological evaluation of NAFLD. Livers of age-matched male WT-STD or WT-HFD mice appeared grossly (data not shown) and histologically normal (**Fig. 1***A*,*B*), where all mice within the same group had very similar patterns of response. In contrast, livers from Null-STD mice were much paler and larger in size compared with those of WT mice. Histological analysis of the Null-STD mice revealed the accumulation of micro-vesicular intracellular lipid droplets (Fig. 1*C*) that were not observed in the WT groups. Livers from Null-HFD mice were even paler than their STD-fed counterparts with accumulated micro- and macro-vesicular lipid droplets, leading to hepatocyte ballooning and steatosis. In addition, displacement of nuclei, collapsed sinusoidal spaces, and inflammatory foci (arrows representing the infiltrated neutrophils) were prominently noted in Null-HFD mice (Fig. 1*D*). The analysis of histological scoring system for NAFLD activity (14) revealed that Null-HFD mice were the only group to achieve the NAS of 5, which differed from the other 3 groups (Fig. 1*E*). Collectively, these results suggest that Null-HFD mice are much more susceptible to the NASH development than the corresponding WT mice, similar to the earlier results (10).

Increased liver:body weight ratio. Weight gain did not differ among the 4 groups of mice (data not shown). However, the ratios of liver:total body weight (liver index) were higher in *Ppara*-null mice than in WT mice ($P < 0.05$) (**Table 1**). The increased liver:body weight ratio in the *Ppara*-null mice could be, at least partly, due to intracellular lipid accumulation, consistent with the previous study with Null-HFD mice (45% energy from fat) fed for 6 mo (10). Plasma alanine aminotransferase (ALT) and aspartate aminotransferase (AST) activities did not differ between *Ppara*-null mice and the WT groups (Table 1), similar to the original report using the same diet (13).

Inhibition of mitochondrial thiolase in Null-HFD mice. Because hepatic fat accumulation could partly result from inhibition of the fat degradation pathways, we evaluated the

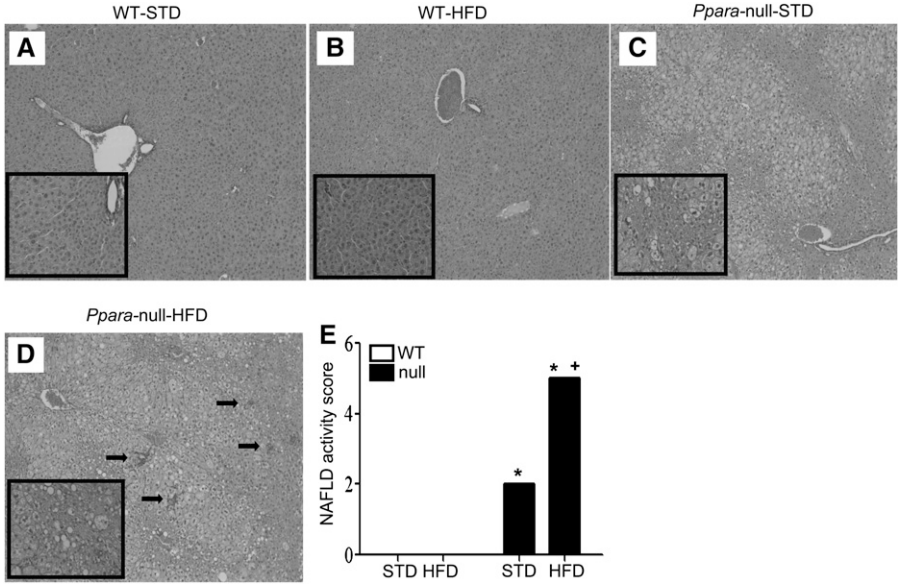

FIGURE 1 Liver histology of WT and *Ppara*-null mice fed STD or HFD for 3 wk (*A–D*). Hematoxylin and eosin stain shows intracellular lipid accumulation and inflammation (200×). The enclosed box in each panel shows the enlarged images (400×) and black arrows (*D*) indicate inflammatory foci. (*E*) Values are means ± SEM, n = 4 or 3 (WT STD). *Different from corresponding WT group, P = 0.05; +different from Null-STD, P = 0.05. A color version of this figure is available online as **Supplemental Figure 2**.

activity of mitochondrial thiolase, the last enzyme in mitochondrial β-oxidation (19). Both thiolase protein levels ($P < 0.0001$) and activity ($P < 0.001$) in *Ppara*-null mice were lower than those in WT mice (**Fig. 2**). These data suggest that the inhibition of mitochondrial thiolase activity in *Ppara*-null mouse groups could partially contribute to the decreased fat oxidation and ultimately the hepatic fat accumulation.

Increased CYP2E1 protein expression in Null-HFD mice. We evaluated the expression levels of cytosolic and mitochondrial CYP2E1 proteins, because CYP2E1, an important source of oxidative stress (20), was increased by a HFD (13). Cytosolic CYP2E1 protein was ~5.3-fold higher in *Ppara*-null mice compared with WT mice ($P < 0.0001$) (**Fig. 3***A*,*B*). Mitochondrial CYP2E1 protein levels were also ~1.7-fold higher in *Ppara*-null mice than in WT mice ($P < 0.001$). In addition, mitochondrial CYP2E1 protein levels in HFD mice were ~1.3-fold higher compared with STD mice ($P < 0.05$) (Fig. 3*C*,*D*). Thus, feeding a HFD or lacking functional PPARα likely results in elevated CYP2E1 levels.

Increased lipid peroxidation in Null-HFD mice. Increased oxidative stress can elevate the level of lipid peroxidation in conditions associated with a HFD and fatty liver (21). Thus, we evaluated a lipid peroxidation marker, MDA, in both cytosol and mitochondria. Cytosolic MDA levels were higher in *Ppara*-null mice than in WT mice (i.e. genotype effect) ($P < 0.0001$) and in HFD-fed mice relative to STD-fed mice (i.e. diet effect) ($P < 0.0001$) (Table 1). In addition, a genotype-diet interaction was observed with MDA levels in Null-HFD mice, which were ~2.3-fold higher than those in WT-STD mice ($P < 0.05$). Moreover, the Null-HFD mice had an ~66% greater cytosolic MDA level increase compared with their STD-fed counterparts ($P < 0.05$). Similarly, WT-HFD mice had ~42% more cytosolic MDA than the corresponding WT-STD mice ($P < 0.05$). Cytosolic MDA levels in Null-HFD were ~64% higher ($P < 0.05$) relative to WT-HFD mice (Table 1). In contrast, mitochondrial MDA levels did not differ among the groups (data not shown). Thus, lipid peroxidation was higher in HFD-fed *Ppara*-null mice relative to the other groups ($P < 0.05$).

Levels of iNOS and protein nitration. The levels of iNOS and protein nitration, important factors in NASH development (21), were elevated in HFD-fed mice (22). Therefore, we evaluated both variables in the cytosol and mitochondria. Cytosolic and mitochondrial iNOS levels had different patterns in all mouse groups upon HFD feeding. The expression of cytosolic iNOS was ~82% greater ($P < 0.005$) in *Ppara*-null mice compared with the levels of the WT mice (**Supplemental Fig. 1***A*,*B*). Interestingly, a genotype-diet interaction was found ($P < 0.001$) and post hoc analysis indicated that Null-HFD or Null-STD mice had mitochondrial iNOS levels ~35 or ~39% lower,

TABLE 1 Body and liver weights, liver MDA, plasma transaminases, mitochondrial Prx-SO3, and TNFα concentrations in WT and *Ppara*-null mice fed STD or HFD for 3 wk[1]

Measurement	WT-STD	WT-HFD	Null-STD	Null-HFD	Two-way ANOVA[2]
Liver, weight, *g/100 g body*	2.87 ± 0.07	3.06 ± 0.08	4.06 ± 0.06	4.55 ± 0.23	G: $P < 0.05$
ALT, *U/L*	36.3 ± 8.95	43.3 ± 6.39	60.7 ± 9.13	38.5 ± 10.0	
AST, *U/L*	147 ± 7.00	158 ± 11.9	189.8 ± 25.8	201 ± 22.9	
Cytosolic MDA,[3] *μmol/L*	4.67 ± 0.07^{c}	6.65 ± 0.56^{b}	6.56 ± 0.39^{b,c}	10.9 ± 0.48^{a}	G, D: $P < 0.0001$; GxD: $P < 0.05$
Mito. Prx-SO3, *% WT-STD*	100 ± 0.57^{b}	98.1 ± 3.82^{b}	102 ± 6.99^{b}	399 ± 19.4^{a}	G, D, GxD: $P < 0.0001$
TNFα, *pg/50 μg protein*	46.8 ± 8.20	104 ± 12.4	67.3 ± 8.93	164 ± 8.20	G: $P < 0.005$ D: $P < 0.0001$

[1] Data are means ± SEM, n = 4 or 3 (WT-STD). Means in a row with superscripts without a common letter differ, $P < 0.05$.
[2] G, genotype; D, diet.
[3] Cytosolic proteins (20 μg/assay) were used to measure MDA levels in different groups.

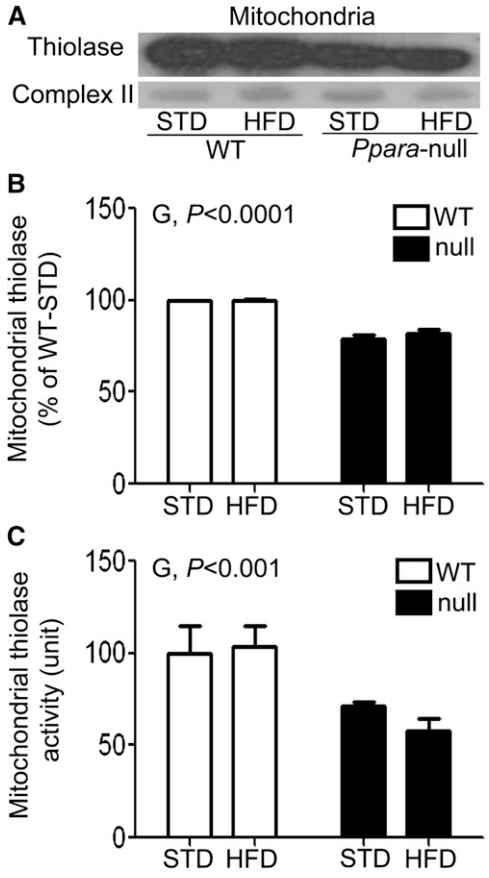

FIGURE 2 Mitochondrial thioase protein (*A*), densitometric levels (*B*), and catalytic activities (*C*) in livers of male WT and *Ppara*-null mice fed STD or HFD for 3 wk. The mitochondrial complex II protein was used to show equal protein loading. Values are means ± SEM, $n = 4$ or 3 (WT-STD). G, genotype.

respectively, than WT-STD mice ($P < 0.05$) and that WT-HFD mice had levels ~64% lower than WT-STD mice ($P < 0.05$) (Supplemental Fig. 1*C*,*D*). In contrast, protein nitration had similar patterns of response in both cytosol and mitochondria. Cytosolic and mitochondrial levels of nitrated proteins were elevated ~61% ($P < 0.01$) and ~53% ($P < 0.0001$), respectively, in *Ppara*-null mice relative to WT mice, while feeding a HFD resulted in decreased cytosolic (31% lower, $P < 0.05$) and mitochondrial (35% lower, $P < 0.0001$) levels of nitrated proteins relative to feeding a STD (Supplemental Fig. 1*E–H*). These data indicate that *Ppara*-null mice had elevated levels of protein nitration compared with WT mice, although the levels of nitrated proteins in STD-fed mice were higher than those of the HFD-fed groups.

Evaluation of a marker for protein oxidation. Prx represent thioredoxin-dependent peroxide reductases that are capable of removing low amounts of peroxides and/or peroxynitrite produced during normal cellular metabolism (23). At least 6 isoforms of Prx have been identified: Prx I, II, and VI are expressed in the cytosol, Prx III is restricted to mitochondria, Prx IV is secreted, and Prx V is located in mitochondria and peroxisomes (23). Upon oxidation, Prx becomes inactivated (23,24). Furthermore, we recently reported increased Prx oxidation and inactivation in conditions associated with increased ROS/RNS production (25). Thus, Prx oxidation (formation of Prx-SO3) was evaluated in both cytosol and mitochondria in all 4 groups (Table 1). Cytosolic Prx-SO3 did not differ among the groups (data not shown), but mitochondrial Prx-SO3 levels were significantly greater in Null-HFD mice than in other groups (Table 1). These results collectively suggest that Null-HFD mice had the highest levels of oxidative stress among all groups.

Increased TNFα in HFD-fed mice. Based on the key role of the proinflammatory cytokine TNFα in NASH models (10,13), the TNFα levels in all groups were determined. Hepatic TNFα levels were ~1.5-fold greater in *Ppara*-null mice compared with WT mice ($P < 0.005$) and ~2.4-fold higher in HFD-fed mice relative to STD-fed mice (Table 1). Thus, the elevated TNFα levels in *Ppara*-null mice and in response to HFD feeding reflect a state of inflammation.

Activation of JNK and p38 kinase in Ppara-null mice. Both ROS/RNS and proinflammatory cytokines such as TNFα can promote the death signaling pathways by activating JNK and p38 kinase (26). The levels of p-JNK (**Fig. 4***A*,*B*) were greater in *Ppara*-null mice relative to WT mice ($P < 0.0001$). Levels of p-p38 kinase were ~3-fold higher in *Ppara*-null mice compared with WT mice ($P < 0.0001$) and ~33% higher in HFD-fed mice

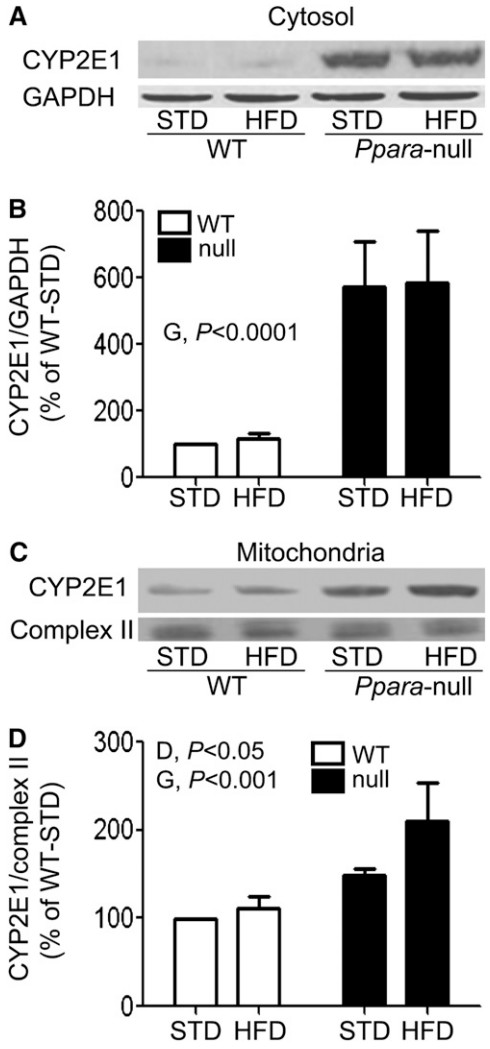

FIGURE 3 Levels of CYP2E1 protein in cytoplasm (*A*) or mitochondria (*C*) in livers of male WT and *Ppara*-null mice fed STD or HFD for 3 wk. The densities measured by immunoblot analysis were normalized to GAPDH (*B*) and complex II subunit (*D*), respectively, and were plotted as a percentage of the value in WT-STD mice. Values are means ± SEM, $n = 4$ or 3 (WT-STD). G, genotype; D, diet.

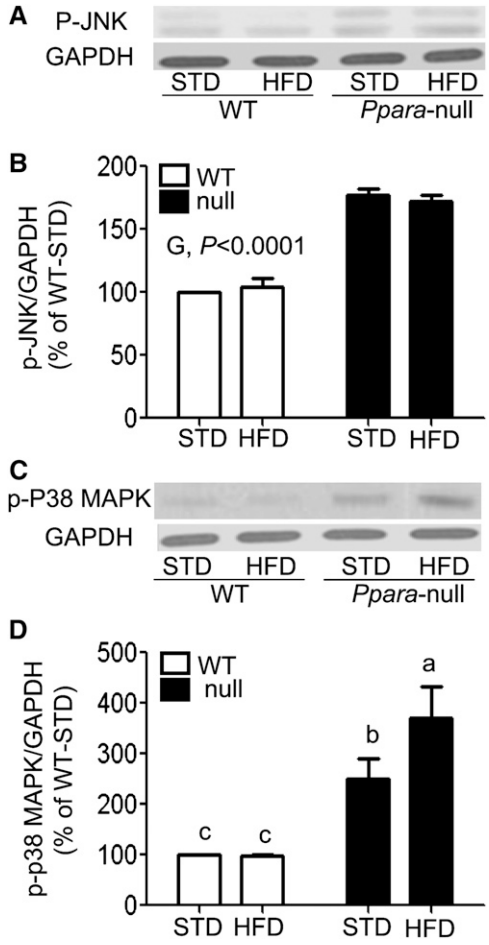

FIGURE 4 Activation of JNK (*A*) or p38 kinase (*C*) in livers of WT and *Ppara*-null mice fed STD or HFD for 3 wk. Cytosolic proteins (100 μg/lane) were used to determine the activation of JNK and p38 kinase. The densities of immunoreactive bands were normalized to GAPDH (*B,D*) and plotted as a percentage of the levels in WT-STD mice. Significance levels are indicated for differences between genotypes (G). Values are means ± SEM, n = 4 or 3 (WT-STD). (*D*) Labeled means without a common letter differ, $P < 0.05$.

compared with STD-fed mice ($P < 0.05$) (Fig. 4*C*,*D*). A genotype-diet interaction was also found ($P < 0.05$). Levels of p-p38 kinase were significantly greater in both *Ppara*-null mouse groups compared with their corresponding WT mice, but the p-p38 kinase level was higher in Null-HFD mice than in all other groups (Fig. 4*C*,*D*).

Increased hepatocyte apoptosis in Null-HFD mice. The activation of JNK and p38 kinase can cause apoptosis and/or necrosis (21,26). HFD also increased JNK activity in rats (21). To demonstrate apoptosis in our groups, a TUNEL assay was performed. TUNEL-positive hepatocytes were readily observed in the Null-HFD mice and were significantly greater in number than in the Null-STD, WT-STD, or WT-HFD groups (**Fig. 5**). These results suggest that increased ROS, together with increased inflammation and subsequent activation of JNK and p38 kinase, likely promote increased apoptosis in Null-HFD mice compared with other groups.

Discussion

Lieber et al. (13) originally reported a new rodent model of NAFLD by providing a liquid HFD containing 71% energy from fat. However, this high-fat liquid diet regimen may have a few disadvantages, such as having a labor-intensive feeding procedure and the fat contents/compositions may not necessarily reflect those in regular American diets. Nonetheless, in this rodent model, rats fed a HFD only for 3 wk developed several key features of NAFLD, such as steatosis, inflammation (with increased levels of TNFα), and increased oxidative stress parameters such as increased CYP2E1 protein and lipid peroxidation, possibly due to extremely high levels of 18:1(n-9) and 18:2(n-6) fatty acids compared with 18:3(n-3) and 22:6(n-3) fatty acids contained in this HFD. Furthermore, this new NASH model also seemed to avoid the nutritional deficiency problem associated with a methionine/choline-deficient diet (27), which does not reflect the conditions of human NASH patients.

PPARα is highly expressed in metabolically active tissues such as heart, kidney, intestinal mucosa, skeletal muscle, brown fat, and liver where it regulates genes involved in lipid metabolism, gluconeogenesis, and amino acid metabolism (5,6). For instance, PPARα directly regulates many genes encoding for the enzymes that are involved in the mitochondrial and peroxisomal fatty acid β-oxidation pathways (5–7). In addition, administration of PPARα agonists ameliorates hepatic steatosis in mice fed a methionine/choline-deficient diet (28). Furthermore, oxidized fat was shown to prevent alcohol-induced TG accumulation through activating PPARα target genes (29). Taken together, it is reasonable to hypothesize that *Ppara*-null mice are more susceptible to NAFLD and NASH compared with WT mice following short-term feeding of a HFD. Thus, we aimed to investigate this hypothesis in *Ppara*-null and WT mice by using the HFD-feeding model for only 3 wk (13) instead of feeding for 6 mo (10).

Our results demonstrated that among all the groups, only the Null-HFD group had extensive lobular inflammation (Fig. 1*D*) and achieved the NAS (Fig. 1*E*) qualified for NASH (14). These results suggest a critical role for PPARα in fat accumulation and concomitant inflammation (NASH development). The increased liver:body weight ratios in *Ppara*-null mice (Table 1) can be explained by accumulation of intracellular lipid droplets, at least partially due to the inhibition of peroxisomal and mitochondrial fatty acid β-oxidation pathways, evidenced by the decreased protein levels and activity of mitochondrial thiolase (Fig. 2). Based on small changes in its protein content, the thiolase activity could be inhibited through oxidative modification (including *S*-nitrosylation) of its active site Cys residues (16) during increased oxidative stress in Null-HFD mice. Thus, the first hit, namely steatosis, of the two-hit theory for NASH development (30) appears to markedly occur in *Ppara*-null mice (**Fig. 6**). Despite no significant differences among the groups (Table 1), the serum transaminase levels are within the normal ranges, as reported (31,32). The basal ALT/AST levels could depend on mouse strains, gender, age, and diet conditions, including diet composition, fat content, feeding duration, etc., which help explain the basal transaminase levels in our current study. It is also true that an underlying hepatic disorder can exist in the absence of elevated serum transaminases, as recently reported (33).

The second hit is lipid peroxidation promoted by the increased oxidative stress produced by various factors, including elevated CYP2E1 and oxidized inactivated Prx. We observed that both cytosolic and mitochondrial CYP2E1, an enzyme known to produce ROS (20) that indirectly forms peroxynitrite through its production of superoxide which interacts with NO (17,34), were elevated in *Ppara*-null mice. Indeed, a pathogenic role for CYP2E1 in both alcoholic steatohepatitis (35) and NASH (21,29,36) has been reported, although other sources of oxidative stress cannot be excluded. The upregulation of CYP2E1

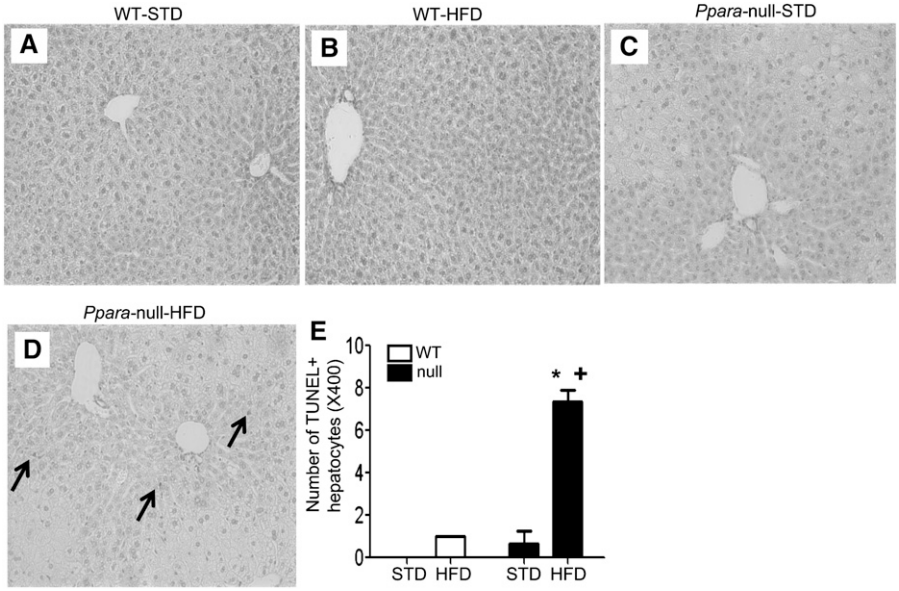

FIGURE 5 Levels of apoptotic hepatocytes (*A-D*) in livers of WT and *Ppara*-null mice fed STD or HFD for 3 wk. TUNEL-positive hepatocytes were identified by black arrows (*D*) and quantified (*E*) in 20 high-power fields (×400). Values are means ± SEM, n = 4 or 3 (WT-STD). *Different from the corresponding WT group, P = 0.05; +different from Null-STD, P = 0.05. A color version of this figure is available online as **Supplemental Figure 3**.

in *Ppara*-null mice may be attributed, at least partly, to the excess fatty acids and ketones that are substrates or inducers of CYP2E1 (35,37). Hepatic steatosis sensitizes the liver, making it susceptible to more serious conditions such as inflammation and fibrosis through the increased production of ROS/RNS and the presence of oxidizable unsaturated fatty acids (22). Oxidation of unsaturated fatty acids contained in corn oil (13) can produce MDA and 4-HNE, both of which can activate hepatic stellate cells, resulting in fibrosis through increased production of collagen and α-smooth muscle actin (38,44). Indeed, the lipid peroxidation levels were highest in Null-HFD mice. Furthermore, the TNFα level, which can be induced by increased oxidative stress, was elevated by feeding a HFD and in *Ppara*-null mice. This fact probably contributes to the lobular inflammation (i.e. fat-induced NASH) observed histologically (Fig. 1), similar to the condition observed in alcoholic steatohepatitis (39).

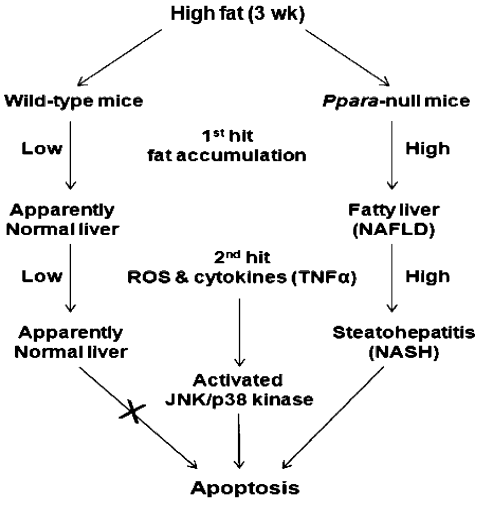

FIGURE 6 A proposed role of PPARα in the development of NAFLD/NASH. The early accumulation of intracellular lipids (first hit) followed by the increased oxidative stress and inflammatory cytokines (second hit), which can activate JNK and p38 kinase, contribute to NAFLD/NASH, and ultimately lead to apoptosis of hepatocytes.

NO and ROS can produce a more potent oxidant peroxynitrite ($ONOO^-$), which plays a key role in the development and/or progression of NASH through nitration of various proteins (40,41). The amount of nitrated proteins, a footprint of peroxynitrite, increased in the liver of obese *ob/ob* mice (41). We found increased amounts of cytosolic iNOS, whereas mitochondrial iNOS levels actually decreased in Null-HFD mice. We are not sure about the reason for this discrepancy. The different levels of antioxidant enzymes and/or the potential negative feedback regulation of iNOS for cell protection may account for different iNOS levels in the cytosol and mitochondria. Alternatively, it is also possible that mitochondrial iNOS was upregulated at earlier time points and then decreased at later time points, as was previously reported (42). We also found that the levels of nitrated proteins were higher in *Ppara*-null mice than in WT mice. The lower levels of nitrated proteins in Null-HFD mice than in the Null-STD mice may be due to increased degradation of nitrated proteins through proteasomes and other proteolytic pathways (43), resulting in shorter half-lives than the native protein counterparts (18,34). Alternatively, the decreased protein nitration in HFD-exposed mice compared with the corresponding STD-fed groups may reflect a negative feedback regulation for this event, similar to that of mitochondrial iNOS. However, further research is needed to investigate the roles and temporal changes in the amounts of nitrated proteins.

The current data collectively provided evidence that both parameters (i.e. fat accumulation and oxidative stress) of the two-hit hypothesis (29) occurred to a stronger extent in Null-HFD mice (Fig. 6). Despite the increase in some indicators of oxidative stress and inflammation in the WT-HFD mice, the increases were minimal and less effective compared with those of the corresponding *Ppara*-null mice. The delayed development of steatohepatitis in the WT mice in our study compared with the rats originally described (13) is unknown and could possibly be due to strain differences.

Both elevated ROS/RNS and proinflammatory cytokines such as TNFα can promote the cell death signaling pathways via activating JNK and p38 kinase, leading to apoptosis and/or necrosis (21,26). Our results of increased hepatocyte apoptosis in Null-HFD mice determined by TUNEL assay (Fig. 5) are in agreement with the earlier results of JNK- and/or p38 kinase-

mediated hepatic apoptosis observed in rats exposed to HFD (21,44). Despite the fact that JNK was also activated in the Null-STD mice, apoptosis was only observed in the HFD-fed group, possibly due to the longer persistence and stronger activation of JNK and p38 kinase in this group than in the STD-fed group.

In summary, this study demonstrated a critical role for PPARα in preventing fat-related oxidative stress, inflammation, and faster development of NAFLD and NASH even after 3 wk of feeding with a HFD. This result was possibly mediated by the earlier development of hepatic steatosis accompanied by the increased levels of ROS/RNS and TNFα in the Null-HFD mice (Fig. 6). Because of the rapid development of NASH (within 3 wk of high-fat feeding), this mouse model may be used for future translational research to identify beneficial agents in efficiently treating and/or preventing NASH.

Acknowledgments

We thank Dr. Nancy Braverman for providing the anti-thiolase antibody. M.A.A. and B.J.S. designed the research; M.A.A., S.H. Y., and L.E.H. conducted the research; M.A.A., F.J.G., K.J.W., and B.J.S. analyzed the data; M.A.A., F.J.G., K.J.W., and B.J.S. wrote the paper; and B.J.S. had primary responsibility for final content. All authors read and approved the final manuscript.

Literature Cited

1. Marchesini G, Bugianesi E, Forlani G, Cerrelli F, Lenzi M, Manini R, Natale S, Vanni E, Villanova N, et al. Nonalcoholic fatty liver, steatohepatitis, and the metabolic syndrome. Hepatology. 2003;37:917–23.
2. Neuschwander-Tetri BA, Caldwell SH. Nonalcoholic steatohepatitis: summary of an AASLD Single Topic Conference. Hepatology. 2003;37: 1202–19.
3. Ruhl CE, Everhart JE. Epidemiology of nonalcoholic fatty liver. Clin Liver Dis. 2004;8:501–19.
4. Adams LA, Lymp JF, St Sauver J, Sanderson SO, Lindor KD, Feldstein A, Angulo P. The natural history of nonalcoholic fatty liver disease: a population-based cohort study. Gastroenterology. 2005;129:113–21.
5. Desvergne B, Wahli W. Peroxisome proliferator-activated receptors: nuclear control of metabolism. Endocr Rev. 1999;20:649–88.
6. Gonzalez FJ, Shah YM. PPARalpha: mechanism of species differences and hepatocarcinogenesis of peroxisome proliferators. Toxicology. 2008;246: 2–8.
7. Aoyama T, Peters JM, Iritani N, Nakajima T, Furihata K, Hashimoto T, Gonzalez FJ. Altered constitutive expression of fatty acid-metabolizing enzymes in mice lacking the peroxisome proliferator-activated receptor alpha (PPARalpha). J Biol Chem. 1998;273:5678–84.
8. Vanden Berghe W, Vermeulen L, Delerive P, De Bosscher K, Staels B, Haegeman G. A paradigm for gene regulation: inflammation, NF-kappaB and PPAR. Adv Exp Med Biol. 2003;544:181–96.
9. Poynter ME, Daynes RA. Peroxisome proliferator-activated receptor alpha activation modulates cellular redox status, represses nuclear factor-kappaB signaling, and reduces inflammatory cytokine production in aging. J Biol Chem. 1998;273:32833–41.
10. Stienstra R, Mandard S, Patsouris D, Maass C, Kersten S, Muller M. Peroxisome proliferator-activated receptor alpha protects against obesity-induced hepatic inflammation. Endocrinology. 2007;148:2753–63.
11. Okiyama W, Tanaka N, Nakajima T, Tanaka E, Kiyosawa K, Gonzalez FJ, Aoyama T. Polyenephosphatidylcholine prevents alcoholic liver disease in PPARalpha-null mice through attenuation of increases in oxidative stress. J Hepatol. 2009;50:1236–46.
12. Abdelmegeed MA, Moon KH, Hardwick JP, Gonzalez FJ, Song BJ. Role of peroxisome proliferator-activated receptor-alpha in fasting-mediated oxidative stress. Free Radic Biol Med. 2009;47:767–78.
13. Lieber CS, Leo MA, Mak KM, Xu Y, Cao Q, Ren C, Ponomarenko A, DeCarli LM. Model of nonalcoholic steatohepatitis. Am J Clin Nutr. 2004;79:502–9.
14. Kleiner DE, Brunt EM, Van Natta M, Behling C, Contos MJ, Cummings OW, Ferrell LD, Liu YC, Torbenson MS, et al. Design and validation of a histological scoring system for nonalcoholic fatty liver disease. Hepatology. 2005;41:1313–21.
15. Suh SK, Hood BL, Kim BJ, Conrads TP, Veenstra TD, Song BJ. Identification of oxidized mitochondrial proteins in alcohol-exposed human hepatoma cells and mouse liver. Proteomics. 2004;4:3401–12.
16. Moon KH, Hood BL, Kim BJ, Hardwick JP, Conrads TP, Veenstra TD, Song BJ. Inactivation of oxidized and S-nitrosylated mitochondrial proteins in alcoholic fatty liver of rats. Hepatology. 2006;44:1218–30.
17. Halliwell B, Chirico S. Lipid peroxidation: its mechanism, measurement, and significance. Am J Clin Nutr. 1993;57 Suppl:S715–25.
18. Abdelmegeed MA, Moon KH, Chen C, Gonzalez FJ, Song BJ. Role of cytochrome P450 2E1 in protein nitration and ubiquitin-mediated degradation during acetaminophen toxicity. Biochem Pharmacol. 2010;79: 57–66.
19. Schulz H. Beta oxidation of fatty acids. Biochim Biophys Acta. 1991; 1081:109–20.
20. Caro AA, Cederbaum AI. Oxidative stress, toxicology, and pharmacology of CYP2E1. Annu Rev Pharmacol Toxicol. 2004;44:27–42.
21. Wang Y, Ausman LM, Russell RM, Greenberg AS, Wang XD. Increased apoptosis in high-fat diet-induced nonalcoholic steatohepatitis in rats is associated with c-Jun NH2-terminal kinase activation and elevated proapoptotic Bax. J Nutr. 2008;138:1866–71.
22. Mantena SK, Vaughn DP, Andringa KK, Eccleston HB, King AL, Abrams GA, Doeller JE, Kraus DW, Darley-Usmar VM, et al. High fat diet induces dysregulation of hepatic oxygen gradients and mitochondrial function in vivo. Biochem J. 2009;417:183–93.
23. Rhee SG, Chae HZ, Kim K. Peroxiredoxins: a historical overview and speculative preview of novel mechanisms and emerging concepts in cell signaling. Free Radic Biol Med. 2005;38:1543–52.
24. Lee YM, Park SH, Shin DI, Hwang JY, Park B, Park YJ, Lee TH, Chae HZ, Jin BK, et al. Oxidative modification of peroxiredoxin is associated with drug-induced apoptotic signaling in experimental models of Parkinson disease. J Biol Chem. 2008;283:9986–98.
25. Kim BJ, Hood BL, Aragon RA, Hardwick JP, Conrads TP, Veenstra TD, Song BJ. Increased oxidation and degradation of cytosolic proteins in alcohol-exposed mouse liver and hepatoma cells. Proteomics. 2006;6:1250–60.
26. Kim BJ, Ryu SW, Song BJ. JNK- and p38 kinase-mediated phosphorylation of Bax leads to its activation and mitochondrial translocation and to apoptosis of human hepatoma HepG2 cells. J Biol Chem. 2006;281: 21256–65.
27. Sahai A, Malladi P, Pan X, Paul R, Melin-Aldana H, Green RM, Whitington PF. Obese and diabetic db/db mice develop marked liver fibrosis in a model of nonalcoholic steatohepatitis: role of short-form leptin receptors and osteopontin. Am J Physiol Gastrointest Liver Physiol. 2004;287:G1035–43.
28. Nagasawa T, Inada Y, Nakano S, Tamura T, Takahashi T, Maruyama K, Yamazaki Y, Kuroda J, Shibata N. Effects of bezafibrate, PPAR pan-agonist, and GW501516, PPARdelta agonist, on development of steatohepatitis in mice fed a methionine- and choline-deficient diet. Eur J Pharmacol. 2006;536:182–91.
29. Ringseis R, Muschick A, Eder K. Dietary oxidized fat prevents ethanol-induced triglyceride accumulation and increases expression of PPARα target genes in rat liver. J Nutr. 2007;137:77–83.
30. Day CP, James OF. Steatohepatitis: a tale of two "hits"? Gastroenterology. 1998;114:842–5.
31. Harrison SD Jr, Burdeshaw JA, Crosby RG, Cusic AM, Denine EP. Hematology and clinical chemistry reference values for C57BL/6 X DBA/2 F1 mice. Cancer Res. 1978;38:2636–9.
32. Iowa State University website: http://www.lar.iastate.edu/index.php?option=com_content&view=article&id=113&Itemid=136.
33. Calvaruso V, Craxi A. Implication of normal liver enzymes in liver disease. J Viral Hepat. 2009;16:529–36.
34. Gow AJ, Farkouh CR, Munson DA, Posencheg MA, Ischiropoulos H. Biological significance of nitric oxide-mediated protein modifications. Am J Physiol Lung Cell Mol Physiol. 2004;287:L262–8.
35. Lieber CS. Cytochrome P-4502E1: its physiological and pathological role. Physiol Rev. 1997;77:517–44.
36. Leclercq IA, Farrell GC, Field J, Bell DR, Gonzalez FJ, Robertson GR. CYP2E1 and CYP4A as microsomal catalysts of lipid peroxides in murine nonalcoholic steatohepatitis. J Clin Invest. 2000;105:1067–75.
37. Yun YP, Casazza JP, Sohn DH, Veech RL, Song BJ. Pretranslational activation of cytochrome P450IIE during ketosis induced by a high fat diet. Mol Pharmacol. 1992;41:474–9.

38. Zern MA, Leo MA, Giambrone MA, Lieber CS. Increased type I procollagen mRNA levels and in vitro protein synthesis in the baboon model of chronic alcoholic liver disease. Gastroenterology. 1985;89: 1123–31.
39. Yin M, Wheeler MD, Kono H, Bradford BU, Gallucci RM, Luster MI, Thurman RG. Essential role of tumor necrosis factor alpha in alcohol-induced liver injury in mice. Gastroenterology. 1999;117:942–52.
40. Fujita K, Nozaki Y, Yoneda M, Wada K, Takahashi H, Kirikoshi H, Inamori M, Saito S, Iwasaki T, et al. Nitric oxide plays a crucial role in the development/progression of nonalcoholic steatohepatitis in the choline-deficient, l-amino acid-defined diet-fed rat model. Alcohol Clin Exp Res. 2010;34 Suppl 1:S18–24.
41. Garcia-Ruiz I, Rodriguez-Juan C, Diaz-Sanjuan T, del Hoyo P, Colina F, Munoz-Yague T, Solis-Herruzo JA. Uric acid and anti-TNF antibody improve mitochondrial dysfunction in ob/ob mice. Hepatology. 2006;44:581–91.
42. Casanovas A, Carrascal M, Abian J, Lopez-Tejero MD, Llobera M. Lipoprotein lipase is nitrated in vivo after lipopolysaccharide challenge. Free Radic Biol Med. 2009;47:1553–60.
43. Ischiropoulos H. Protein nitration-An update. Arch Biochem Biophys. 2009;484:117–21.
44. Li SY, Liu Y, Sigmon VK, McCort A, Ren J. High-fat diet enhances visceral advanced glycation end products, nuclear O-Glc-Nac modification, p38 mitogen-activated protein kinase activation and apoptosis. Diabetes Obes Metab. 2005;7:448–54.